

EFFECT OF PHOSPHORUS ADDITION ON THE IMPACT FRACTURE BEHAVIOUR OF Cr-Mo PREALLOYED SINTERED STEELS

H. Danninger, C. Gierl-Mayer, M. Jaliliziyaean
Dedicated to Prof. Dr. Brigitte Weiss, Vienna

Abstract

Phosphorus is known to be a sintering enhancer, being used e.g. to sinter alloy steels in belt furnaces. On the other hand, P is known to cause embrittlement, although this effect is usually much less pronounced with sintered steels than with wrought ones. In the present study, the effect of phosphorus addition on the mechanical behaviour of Cr-Mo prealloy steel grades with varying alloy element content was investigated, both as sintered and sinter hardened variants being tested. It showed that higher Cr and P contents result in better sinter hardening effect, but at the expense of the ductility, for the 3% Cr materials the impact energy dropping even at moderate P levels while the 1.5% Cr variant tolerates higher P contents before embrittlement occurs. Fractography showed that in the as sintered state, addition of P promotes transformation from ductile rupture to cleavage fracture while after sinter hardening pronounced intergranular failure is observed, in particular with the higher Cr alloyed grade. This confirms the results of previous studies with Mo alloy steels that embrittlement is caused by interaction of alloy element and P, apparently by exceeding the solubility product, although the mechanism of embrittlement by faster cooling still has to be explained.

Keywords: *sintered steel, Cr alloying, phosphorus, sinter hardening, embrittlement*

INTRODUCTION

While in wrought steels phosphorus is regarded as a highly unwelcome, heavily embrittling element, it is much less critical in ferrous powder metallurgy [1, 2]. In contrast, P is used as a sintering activator to a considerable extent, both in soft magnetic materials where it promotes shrinkage and pore rounding, thus improving the magnetic properties [3] and in structural steels in which case it enables sintering at lower temperatures without loss of mechanical properties. Phosphorus is a strong ferrite stabilizer, thus enhancing self-diffusion of iron and also heterodiffusion of other elements (which is also faster in ferrite than in austenite), and in particular in the case of rapid heating forms a transient liquid phase which also promotes sintering. The positive effect of P alloying on both strength and ductility of sintered steels is also explained by selective strengthening of the sintering contacts [2, 4], thus resulting in larger deformed areas and ensuing higher elongation values [5].

On the other hand, however, also in sintered steels embrittlement caused by P addition has been reported. This occurs e.g. at high P levels; typically 0.45 mass% P is regarded as the safe limit while at higher levels the tendency to intergranular failure increases, as shown by Auger electron spectroscopy (AES) this is caused by P segregation to the grain boundaries (e.g. [6, 7]). Furthermore, also negative interactions between phosphorus and refractory metals used for alloying have been reported that resulted in embrittlement if the combination between alloy element and P contents exceeded a certain level [8, 9].

Recently, prealloyed steel powders have found widespread applications for manufacturing of sintered steel precision parts. This holds in particular for low Mo alloyed grades which are used for surface densified gears [10] but also Cr and Cr-Mo prealloyed grades. These are more difficult to sinter, because of the higher sensitivity to oxidizing impurities in the atmosphere as well as the difficulty to reduce the oxides present on the powder surfaces [11, 12]. Generally, high sintering temperatures are recommended here to fully exploit the mechanical properties, both regarding the more favourable thermodynamic conditions for carbothermic reduction of the surface oxides and for exploiting the higher sintering activity of the Cr prealloyed steels compared to unalloyed or Mo alloyed grades, as evident from the more pronounced shrinkage.

At least for the latter purpose, P addition might also be helpful, enabling use of lower sintering temperatures for the same interparticle strength. On the other hand, the adverse interactions between Cr and P should not be ignored that were described in [8]. Although in this earlier study Cr had been introduced as elemental powder, i.e. with higher chemical activity, joint segregation of Cr (and if present, Mo) and P to the grain boundaries could not be excluded, at least at higher P levels. In the present study, compacts from Cr and Cr-Mo prealloyed steel powders with varying levels of C and P were investigated with regard to sintering response and mechanical, in particular fracture, behaviour. Since it had been found [8, 9] that Mo and P combined with carbon resulted in sinter hardening behaviour, also sinter hardening tests were done.

EXPERIMENTAL TECHNIQUE

The starting powders used were water atomized grades AstaloyCrL (Fe-1.5%Cr-0.2%Mo) and AstaloyCrM (Fe-3.0%Cr-0.5%Mo) from Hoganas AB, Sweden. Natural graphite UF4 was used as carbon carrier, the nominal combinations being AstaloyCrL-0.6%C and AstaloyCrM-0.5%C (all data in mass%), and the P source was fine Fe₃P powder obtained from MIBA Sinter Austria GmbH. The powders were mixed in a tumbling mixer for 60 min and then compacted at 600 MPa to impact test bars ISO 5754 (55 x 10 x 10 mm), a pressing tool with floating die being used.

The first batch of specimens was used for dilatometric runs; here, 0.45% P were added, and P-free reference materials were also prepared. The powder mixes were pressed with die wall lubrication, sizing oil Multical being used. The green bodies were then sintered in a pushrod dilatometer (Netzsch 402L) with Al₂O₃ measuring system in different high purity atmospheres (H₂ and Ar, all of 5.0 grade = 99.999% purity). The parameters for the dilatometric runs were as follows: Heating 10 K/min, T_{max} = 1300°C, held for 60 min isothermal soaking, cooling -10 K/min. 1300°C was selected as standard sintering temperature for Cr-Mo prealloyed grades, granting complete deoxidation.

For the second batch, specimens with varying P content were prepared. Once more, pressing was done at 600 MPa with die wall lubrication. In this case the green bodies were sintered for 60 min at 1250°C in a push-type furnace with superalloy retort in flowing

high purity H_2 (5.0 quality). This furnace was equipped with a gas-quench unit at one end; gas quenching with N_2 5.0 was done in some runs.

The specimens were characterized following the standard techniques: sintered density according to the water displacement method, dimensional change taking the bar length as a basis; Vickers hardness HV30; Charpy impact testing on a Wolpert tester with $W_{max} = 50$ J. Metallographic preparation was done by standard grinding and diamond polishing with subsequent Nital etching; the fracture surfaces were studied in a scanning electron microscope FEI Quanta 200 in the secondary electron mode.

EXPERIMENTAL RESULTS

Dilatometric studies

The dilatometric graphs clearly reveal the effect of P addition on the dimensional behaviour of the Cr-Mo steels. In Figure1 the graphs are shown for CrL-0.6%C(-0.45%P), in Fig.2 the respective graphs for CrM-0.5%C(-0.45%P) are shown.

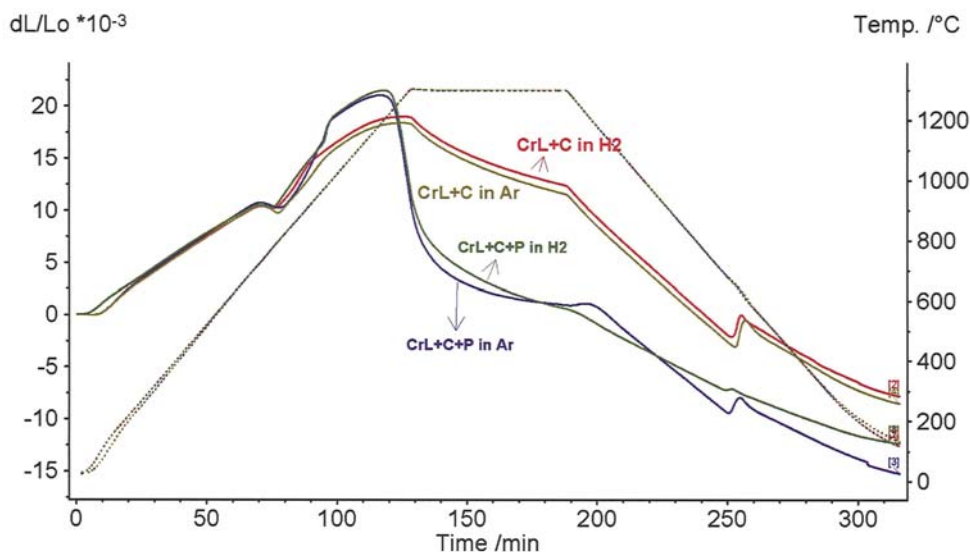


Fig.1. Dilatometric graphs of AstaloyCrL-0.6%C(-0.45%P) sintered in H_2/Ar respectively. 10 K/min / 60 min 1300°C / -10 K/min.

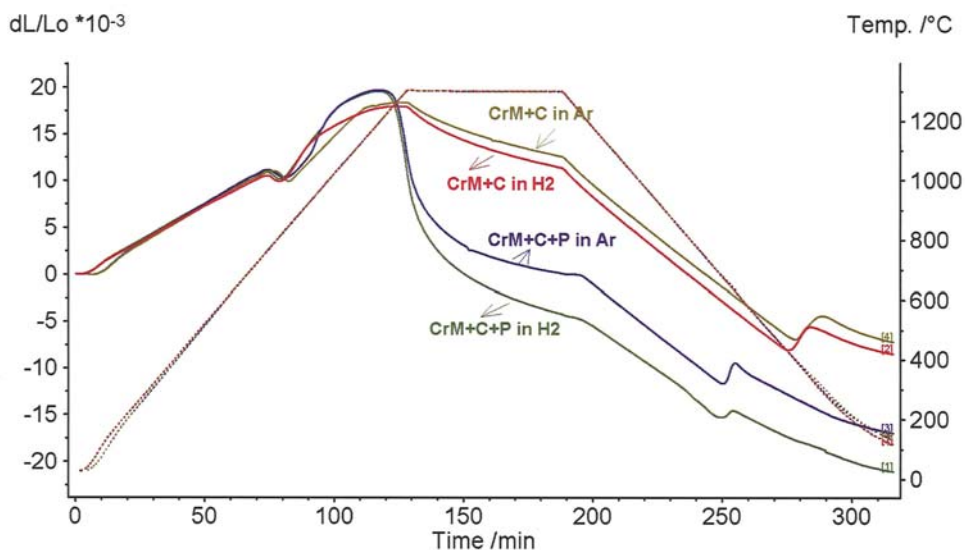


Fig.2. Dilatometric graphs of AstaloyCrM-0.6%C(-0.45%P) sintered in H₂/Ar respectively. 10 K/min / 60 min 1300°C / -10 K/min.

For both materials it is evident that the atmosphere – reducing vs. inert – does not play a significant role on the dimensional behaviour, in contrast to the phosphorus content. P containing specimens tend to expand slightly more during heating compared to the P-free reference specimens but mainly in the temperature “window” 900 ... 1000°C. Then the expansion decreases, approximating that of the reference, and from about 1200°C pronounced shrinkage occurs - indicating formation of persistent liquid phase - that continues up to about 20 min isothermal sintering; this effect is not recorded with the P-free reference specimens. Then the shrinkage rate once more approximates that of the reference materials. During cooling it is evident that the CrL based materials show the transformation at about 600°C, i.e. in the pearlite range, while the CrM based ones transform at markedly lower temperatures, at about 400°C, but only the P-free reference material; the 0.45%P grade transforms at 600°C, which can be attributed to the ferrite stabilizing effect of P.

The properties of the specimens sintered in the dilatometer are given in Table 1. As can be clearly seen, the data for the sintered density and the dimensional change mirror the dilatometric graphs. While the P-free reference materials show a dimensional change of about 0.7 .. 1.0% linear, the P containing steels show shrinkage in the range of 1.8 ...2.2%, H₂ atmosphere resulting in slightly higher values than Ar. This is also mirrored in the density values; here, the trapping of Ar in closed pores inhibits densification to degrees possible in H₂.

The hardness is generally below 280 HV10, which means that there were no sinter hardening effects, as was expected from the composition (and the fairly low cooling rate) and also from the dilatometric graphs. The hardness is markedly increased by the introduction of P, more so with the lower Cr-Mo alloyed grade CrL than with CrM, which however shows the higher absolute values. The price to be paid for the higher hardness is however a drastic decrease in impact toughness; in the case of CrL the impact energy decreases from >30 J to <5 J by introduction of 0.45%P, despite the in part high density. With CrM the difference is not quite as pronounced, but also here a marked loss of ductility

can be recorded. This indicates that the negative interaction between P and VIa alloy elements occurs also with Cr-Mo prealloyed materials.

Tab.1. Properties of AstaloyCrL/CrM-C(-P) specimens compared at 600 MPa and sintered in the dilatometer in different atmospheres. 10 K/min / 60 min 1300°C / -10 K/min.

Material	P content [mass %]	Atmo-sphere	Sintered density [$\text{g}\cdot\text{cm}^{-3}$]	Dimensional change [% linear]	Hardness HV10	Impact energy [$\text{J}\cdot\text{cm}^{-2}$]
AstaloyCrL-0.6%C	0.0	H ₂	7.16	-0.86	175	46.0
	0.0	Ar	7.16	-0.93	167	32.2
	0.45	H ₂	7.62	-2.17	223	2.5
	0.45	Ar	7.23	-1.89	262	4.2
AstaloyCrM-0.5%C	0.0	H ₂	7.06	-0.82	241	24.3
	0.0	Ar	7.01	-0.69	250	31.3
	0.45	H ₂	7.30	-2.36	275	4.2
	0.45	Ar	7.21	-1.89	249	11.0

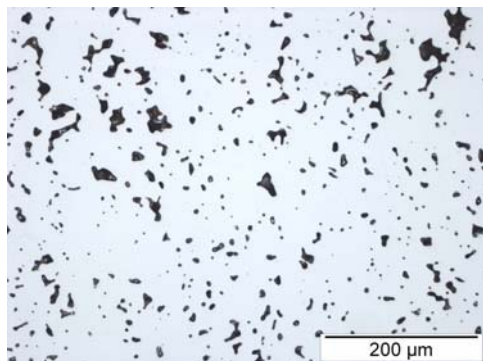


Fig.3a. AstaloyCrL-0.6%C

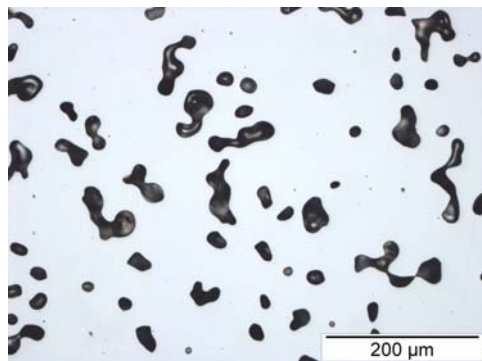


Fig.3b. AstaloyCrL-0.6%C-0.45%P

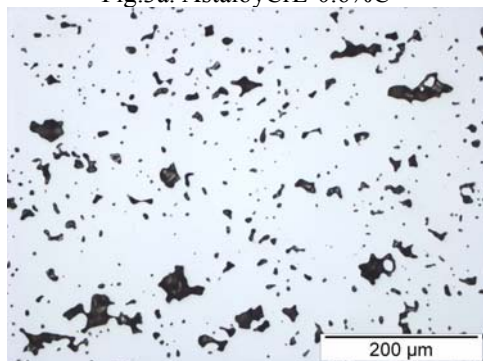


Fig.3c. AstaloyCrM-0.5%C

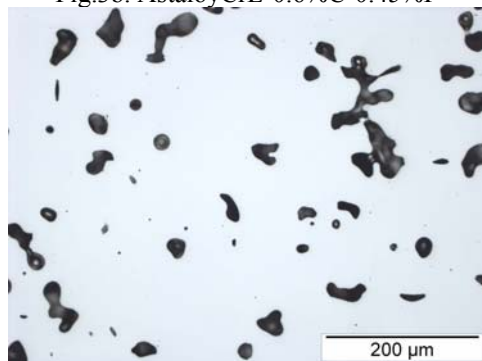


Fig.3d. AstaloyCrM-0.5%C-0.45%P

Fig.3. Metallographic sections of dilatometric specimens sintered in H₂. 10 K/min / 60 min 1300°C / -10 K/min. Unetched.

Metallographic investigations showed the significant activating effect of the P addition. In Figure 3 the pore structure is depicted, and the pronounced pore coarsening caused by phosphorus is clearly evident. Of course the sintering temperature of 1300°C is very high regarding the P content of 0.45%, and the specimens thus must be defined as being oversintered. This also helps to explain the fairly poor impact energy.

The matrix microstructures do not differ too much as a function of P content and atmosphere (Fig.4, 5), as also indicated by the fairly similar temperature intervals for the austenite-ferrite transformation. The exception is CrM-C (without P), which exhibits rather bainitic microstructures, as indicated by the lower transformation temperature. Traces of phosphide eutectic are locally visible in the CrL-C-P specimens, which might also contribute to the poor impact behaviour. According to [13], at these C and P levels a binary eutectic austenite + (Fe,Cr)₃P is to be expected; SEM-EDX and XRD analyses are currently in progress to check this hypothesis. ThermoCalc calculations have indicated that in the eutectoid range there is a transformation from austenite + (Fe,Cr)₃P to Ferrite + (Fe,Cr)₃C, which agrees with the appearance of the microstructure.

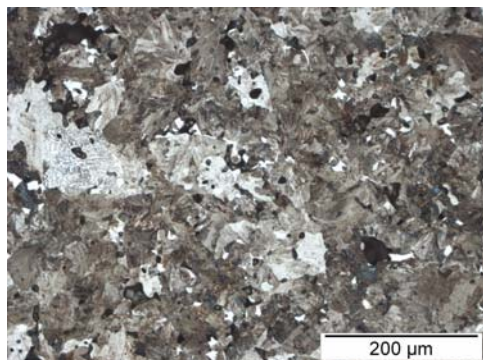


Fig.4a. AstaloyCrL-0.6%C, H₂

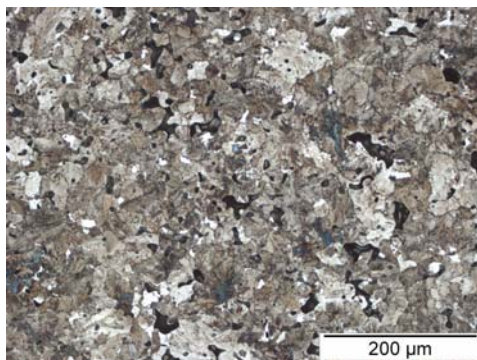


Fig.4b. AstaloyCrL-0.6%C, Ar

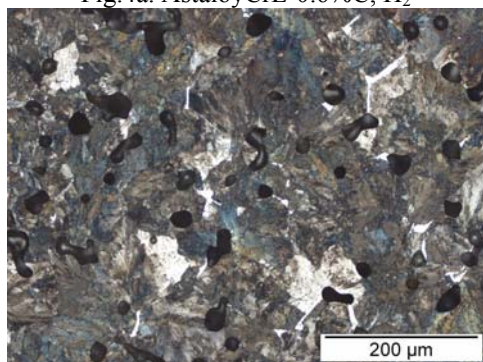


Fig.4c. AstaloyCrL-0.6%C-0.45%P, H₂

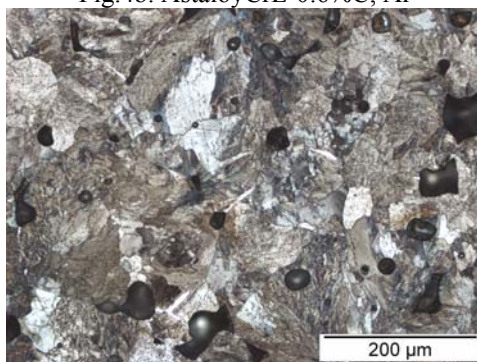


Fig.4d. AstaloyCrL-0.6%C-0.45%P, Ar

Fig.4. Metallographic sections of dilatometric specimens AstaloyCrL-0.6%C(-0.45%P) sintered in H₂/Ar respectively. 10 K/min / 60 min 1300°C / -10 K/min. Nital etched.

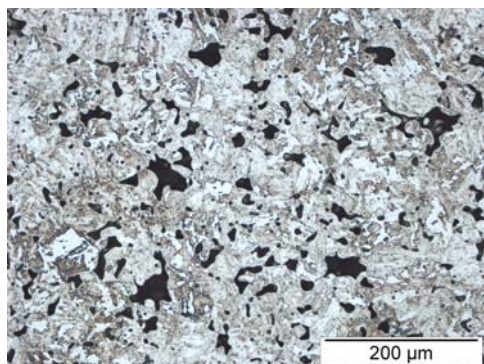
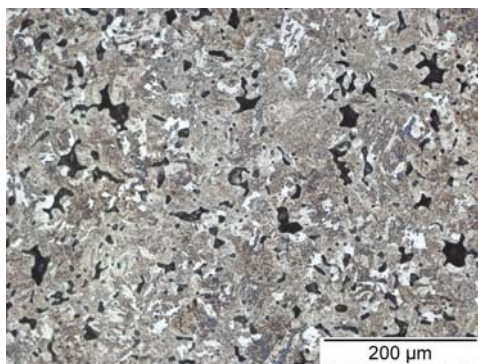
Fig.5a. AstaloyCrM-0.5%C, H₂

Fig.5b. AstaloyCrM-0.5%C, Ar

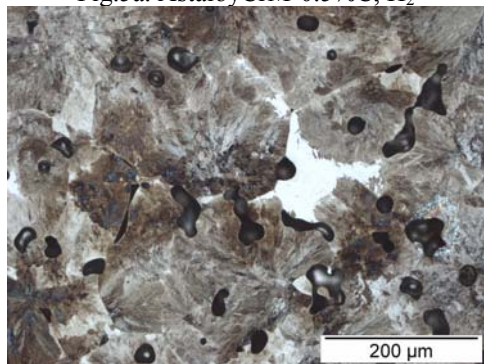
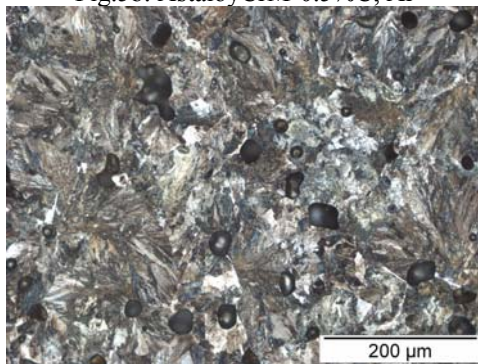
Fig.5c. AstaloyCrM-0.5%C-0.45%P, H₂

Fig.5d. AstaloyCrM-0.5%C-0.45%P, Ar

Fig.5. Metallographic sections of dilatometric specimens AstaloyCrM-0.5%C(-0.45%P) sintered in H₂/Ar respectively. 10 K/min / 60 min 1300°C / -10 K/min. Nital etched.

The impact fracture surfaces were investigated by SEM; typical fractographs are shown in Fig.6. As can be seen, the failure mode of the P-free materials is generally ductile rupture, with the typical dimple structure. The P alloyed specimens, in contrast, exhibit consistently cleavage fracture; surprisingly, there is no intergranular fracture which would be the typical failure mode expected with phosphorus-alloyed sintered steels [7, 9]. This indicates that the reason for the poor impact energy is rather the pronounced microstructural coarsening – as visible from the pores and the size of the cleavage areas - than interfacial embrittlement.

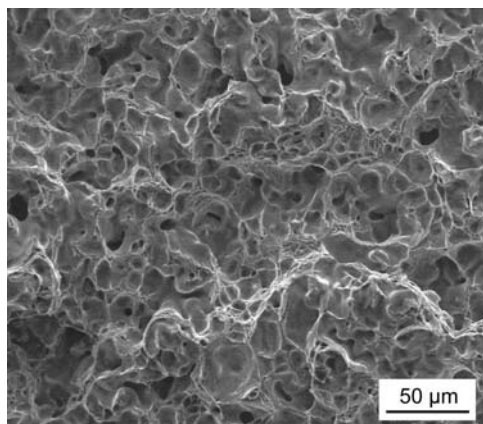


Fig.6a. AstalloyCrL-0.6%C, H₂

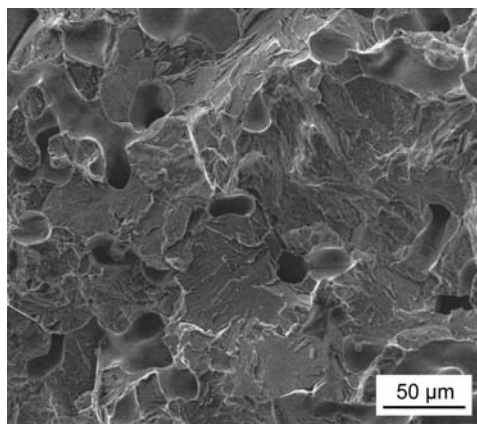


Fig.6b. AstalloyCrL-0.6%C-0.45%P, H₂

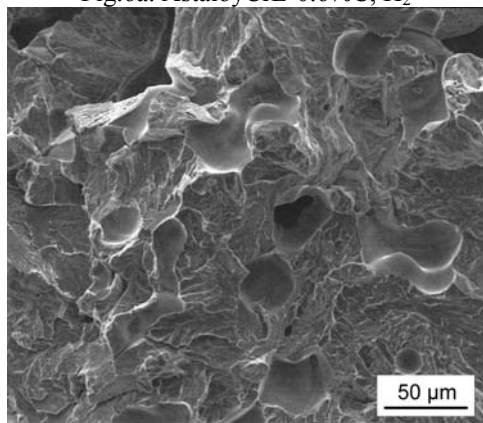


Fig.6c. AstalloyCrL-0.6%C-0.45%P, Ar

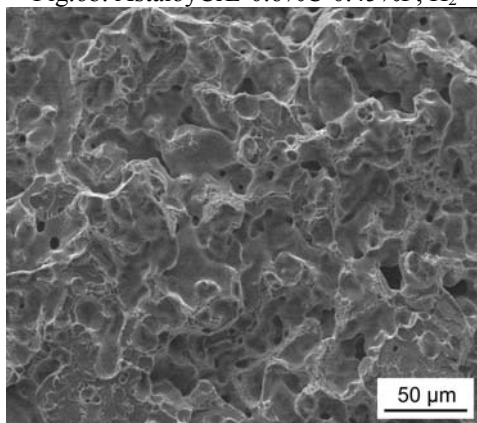


Fig.6d. AstalloyCrM-0.5%C, H₂

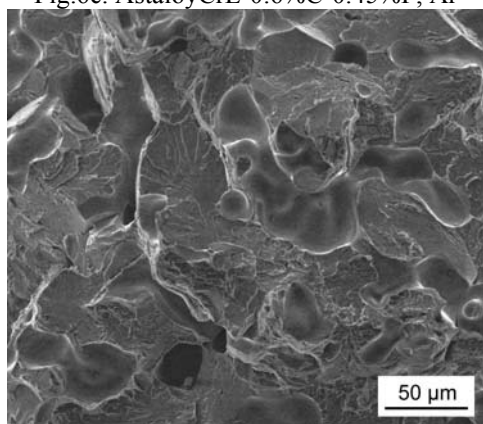


Fig.6e. AstalloyCrM-0.5%C-0.45%P, H₂

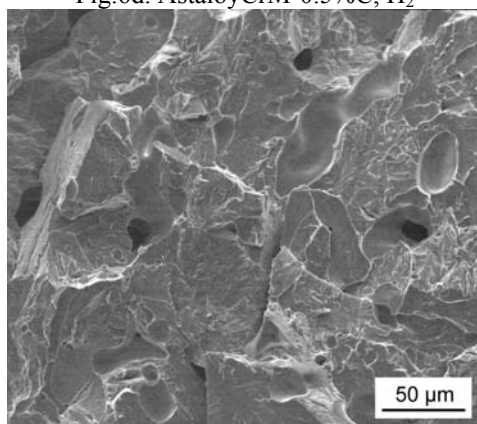


Fig.6f. AstalloyCrM-0.5%C-0.45%P, Ar

Fig.6. Impact fracture surfaces (room temperature) of dilatometric specimens CrL/CrM-C(-P), sintered in H₂/Ar respectively. 10 K/min / 60 min 1300°C / -10 K/min.

Specimens with varying phosphorus content

The results shown so far have clearly indicated that the combination of the selected P content of 0.45% and the sintering temperature of 1300°C was not well suited for this type of materials. Therefore, in a further study specimens with varying P content 0 ... 0.60% (in 0.15% steps) were prepared; the sintering temperature was set at 1250°C, the atmosphere being H₂ grade 5.0. In part the specimens were cooled in H₂ by pushing the boat into the water-jacketed exit zone of the furnace; in part the boat was pushed into the rapid-quench end of the furnace and cooled by flowing N₂. The flow rate was set such as to cause a linearized cooling rate (900 ... 300°C) of about 2 K.s⁻¹, as indicated by a thermocouple in a dummy specimen. In Table 2 the results for the as-sintered materials are shown and in Table 3 those for the sinter hardened ones.

Tab.2. Properties of AstaloyCrL/CrM-C(-P) specimens sintered in the pushtype furnace. Compacted at 600 MPa, sintered 60 min at 1250°C in H₂.

Material	P content [mass %]	Sintered density [g·cm ⁻³]	Dimensional change [% linear]	Hardness HV10	Impact energy [J·cm ⁻²]
AstaloyCrL-0.6%C	0.00	7.08	-0.50	179	21.8
	0.15	7.02	-0.33	183	35.2
	0.30	6.95	-0.20	167	24.1
	0.45	6.90	-0.06	219	17.7
	0.60	6.98	-0.59	205	7.3
AstaloyCrM-0.5%C	0.00	6.99	-0.43	287	15.8
	0.15	6.96	-0.43	288	21.4
	0.30	6.90	-0.25	225	17.6
	0.45	6.83	-0.32	217	16.7
	0.60	6.94	-0.84	223	3.2

Tab.3. Properties of AstaloyCrL/CrM-C(-P) specimens sinter hardened in the pushtype furnace. Compacted at 600 MPa, sintered 60 min at 1250°C in H₂, sinter hardened at 2 K·s⁻¹ in N₂.

Material	P content [mass %]	Sintered density [g·cm ⁻³]	Dimensional change [% linear]	Hardness HV10	Impact energy [J·cm ⁻²]
AstaloyCrL-0.6%C	0.00	7.08	-0.54	191	25.9
	0.15	7.01	-0.33	226	23.9
	0.30	6.94	-0.11	205	16.4
	0.45	6.85	-0.13	313	6.4
	0.60	6.93	-0.30	352	4.1
AstaloyCrM-0.5%C	0.00	6.98	-0.50	355	28.8
	0.15	6.95	-0.52	368	7.4
	0.30	6.88	-0.30	432	3.2
	0.45	6.81	-0.21	461	3.2
	0.60	6.94	-0.57	447	2.4

As can be seen the sintered density values are slightly lower than for the dilatometric specimens in the case of the P-free materials but markedly lower for the P-containing steels. This is surely to some extent a consequence of the lower sintering temperature, but it can also be taken as an indicator for the formation of transient liquid phase which will result in expansion as known from copper [1, 14, 15] but also Mo, Cr and W [16]. The fact that the density – and also the shrinkage – decreases up to 0.45% P and then, at 0.6% P, increases indicates that at this latter P level persistent liquid phase is formed that enhances densification, as shown in the dilatometric runs for the lower P content (0.45%) but at higher isothermal temperature. The sinter hardened specimens show very slightly lower density, which can be explained by the formation of martensitic structures.

The hardness shows a fairly surprising trend: while for the lower alloyed CrL it increases with higher phosphorus content, with the higher alloyed CrM there is a drop in hardness. As indicated by the dilatometric graphs, this can be explained by the earlier transformation as a consequence of the ferrite stabilization by phosphorus. This hypothesis is also supported by metallographic investigations and the hardness data for the sinter hardened materials: here also for CrM higher P content results in at least slightly higher hardness.

The most pronounced effect of the sinter hardening treatment is observed for the impact energy: for the as-sintered materials a fairly regular behaviour is recorded (see Fig.7), with some improvement at low to moderate P contents, indicating a favourable combination of P content and sintering temperature, and impact energy drops significantly only at P contents of 0.6%. Sinter hardening, in contrast, seems to “sensitize” the materials; in particular for the higher alloyed CrM even as low a P content as 0.15% P results in an impact energy well below 10 J·cm⁻², which cannot be explained by any according increase of the hardness.

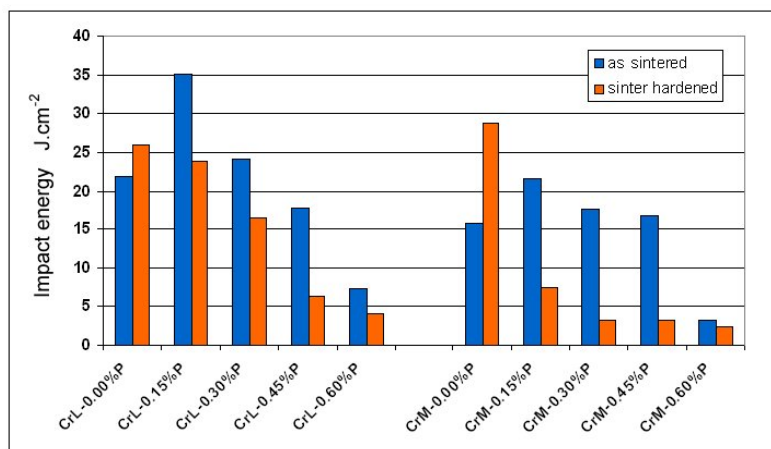


Fig.7. Charpy impact energy of AstaloyCrL/CrM-C(-P) specimens sintered/sinter hardened in the push-type furnace. Compacted at 600 MPa, sintered 60 min at 1250°C in H₂, sinter hardened at 2 K·s⁻¹ in N₂.

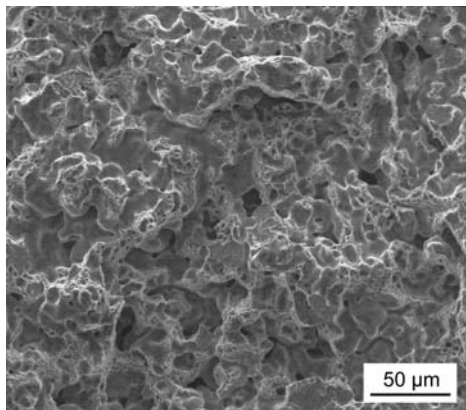


Fig.8a. AstaloyCrL-0.6%C, as sintered

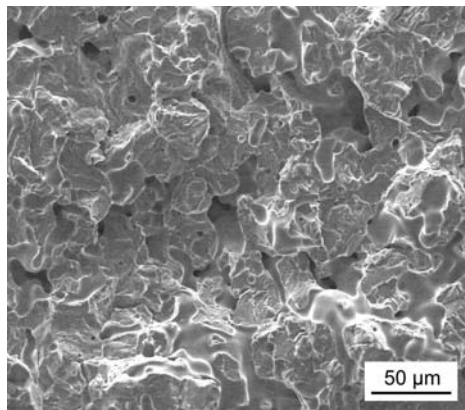


Fig.8b. AstaloyCrL-0.6%C-0.45%P, as sintered

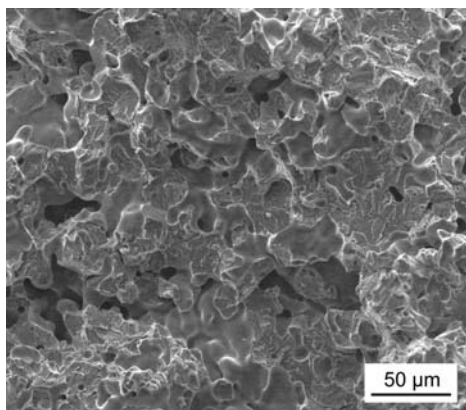


Fig.8c. AstaloyCrM-0.5%C-0.45%P, as sintered

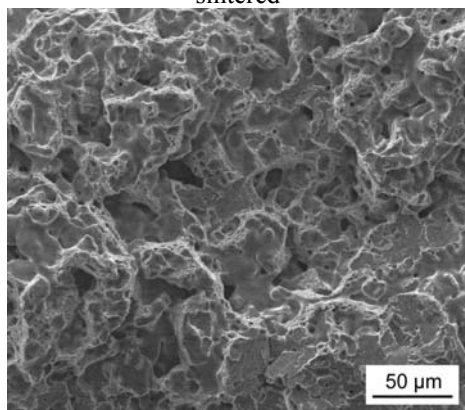


Fig.8d. AstaloyCrL-0.6%C, sinter hardened

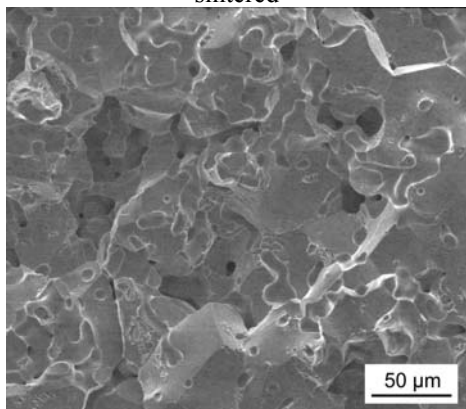


Fig.8e. AstaloyCrL-0.6%C-0.45%P, sinter hardened

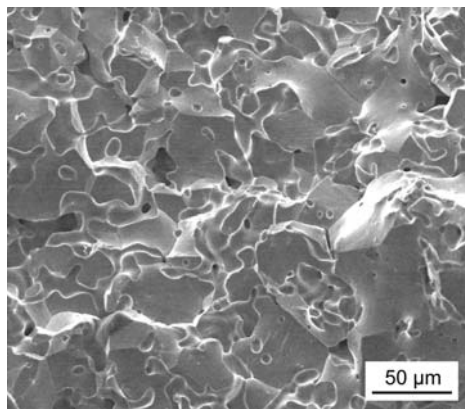


Fig.8f. AstaloyCrM-0.5%C-0.45%P, sinter hardened

Fig.8. Charpy impact fracture surfaces of AstaloyCrL/CrM-C(-P) specimens sintered/sinter hardened in the pushtype furnace. Compacted at 600 MPa, sintered 60 min at 1250°C in H₂, sinter hardened at 2 K·s⁻¹ in N₂.

This behaviour can be explained by fractographic investigations: while the P-free variants exhibit predominantly dimple fracture both as-sintered and sinter hardened, with only a few cleavage fracture surfaces, the P alloyed variants exhibit increasing amounts of transgranular cleavage, which absolutely dominates at P levels of 0.30% and above, but only in the as-sintered state: in the case of sinter hardening there is virtually complete intergranular failure, as visible in Figs.8e, f. The reason for this surprising behaviour is not yet clear; it would be expected that P segregation is more pronounced in the case of slower cooling, but in the present study the reverse has been found. Currently, AES investigations are being done to check if the intergranular fracture can be related to P contamination of the interfaces.

CONCLUSIONS

The experiments have shown that there is a distinct correlation between P content, alloy metal (Cr-Mo) content and sintering temperature. At 1300°C, both AstaloyCrL-0.6%C and CrM-0.5%C exhibit standard solid state sintering while addition of 0.45% P results first in expansion during heating and then in pronounced shrinkage, indicating first transient and then persistent liquid phase. At this P content, 1300°C is definitely too high, resulting in microstructural coarsening and fairly low impact energy values, although the fracture mode is transgranular cleavage and not, as might be expected, intergranular.

Experiments with varying P content have shown that small amounts of P can enhance sintering and result in better mechanical properties; at higher P levels the hardness increases but the impact energy drops. This holds however only for the as sintered state; sinter hardening results in transformation of the fracture mode from transgranular cleavage to intergranular brittle failure, with resulting very poor impact energy values. The reason for this surprising effect of faster cooling is not clear at the moment; detailed chemical analysis is required to reveal if P segregation is responsible here.

Acknowledgement

The authors wish to thank MIBA Sinter Austria GmbH, Vorchdorf, for supplying the starting materials used and Raquel de Oro Calderon, Gothenburg, for the thermodynamic calculations.

REFERENCES

- [1] Lenel, FV.: Powder Metallurgy – Properties and Applications. Princeton NJ : MPIF, 1980
- [2] Šalák, A.: Ferrous powder metallurgy. Cambridge : CISP, 1995
- [3] Jangg, G., Drozda, M., Danninger, H., Eder, G.: Powder Metall. Int., vol. 16, 1984, p. 264
- [4] Miškovič, V., Šlesár, M. In: Proc. 5th Int. Conf. on PM in Czechoslovakia. Vol. 2. Gottwaldov, 1978, p. 47
- [5] Cope, LH.: Metallurgia, vol. 72, 1965, p. 165
- [6] Kreçar, D., Vassileva, V., Danninger, H., Hutter, H.: Anal. Bioanal. Chem., vol. 379, 2004, p. 610
- [7] Vassileva, V., Danninger, H., Kreçar, D., Hutter, H. In: Proc. EuroPM2005, Prague. Vol. 1. Shrewsbury : EPMA, 2005, p. 53
- [8] Üregen, B.: Diploma thesis. TU Wien, 1997
- [9] Danninger, H., Üregen, B. In: Proc. “EURO PM’97” 1997 Europ. Conf. on Adv. In Structural PM Component Production, Munich, Germany. Shrewsbury : EPMA, 1997, p. 319

- [10] Sandner, C., Dickinger, J., Rößler, H., Orth, P. In: Proc.PM2004 World Congress, Vienna. Vol. 5. Eds. H. Danninger, R. Rätzl. Shrewsbury : EPMA, 2004, p. 657
- [11] Karlsson, H., Nyborg, L., Berg, S., Yu, Y. In: Proc. EuroPM2001 Nice. Vol. 1. Shrewsbury : EPMA, 2001, p. 22
- [12] Hryha, H., Nyborg, L., Gierl, C., Danninger, H., Bengtsson, S. In: Proc. PM2010 Powder Metallurgy World Congress and Exhibition, Florence. Vol. 1. Shrewsbury : EPMA, 2010, p. 25
- [13] Raghavan, VG.: Phase Diagrams of Ternary Iron Alloys Part 3: Ternary Systems Containing Iron and Phosphorus. Calcutta : Indian Inst, of Metals, 1988
- [14] Dautzenberg, N., Dorweiler, HJ.: Powder Metall. Int., vol. 17, 1985, no. 6, p. 279
- [15] Tabeshfar, K., Chadwick, GA.: Powder Metall., vol. 27, 1984, p. 19
- [16] Danninger, H., Pöttschacher, R., Bradac, S., Šalák, A., Seyrkammer, J.: Powder Metall., vol. 48, 2005, no.1, p. 23